

DYNAMIC MODELING OF SPACECRAFT WITH FLEXIBLE MEMBRANE

Matthew Brownell*, Andrew J. Sinclair†, Puneet Singla‡

The main focus of this work is to derive a mathematical model for a conceptual design of a large solar-powered spacecraft. The spacecraft is considered to be a flexible membrane clamped within a rigid, rectangular frame. The structure is motivated by a concept for capturing solar energy in space and accurately directing it to required locations on the Earth's surface. Simulation results provide useful information for the vibrations this type of spacecraft will experience in orbit. In subsequent work, we wish to utilize this model to develop data-driven modeling techniques to be used with real-time spacecraft input-output data.

INTRODUCTION

The accurate and timely supply of energy for the Department of Defense is paramount to mission success. Space solar power is one concept to address this need via capturing solar energy in space and accurately directing it to required locations on the Earth's surface. To achieve this mission, deployable structures with large apertures have been considered; however, to accurately transmit power, precise knowledge of the dynamic shape of the large flexible structure is required. Additionally, vibrations of the structure are of great interest and must be minimized in order to maintain pointing accuracy.¹ One concept to measure the structural shape is to distribute sensors over the surface that provide local displacement or slope information. This local data can be used to estimate the shape of the spacecraft and therefore apply corrections to the radio-frequency beam formation. Whereas algebraic "curve fitting" may be used to find the amplitudes of a set of basis functions, system identification finds a dynamical model solution for the input-output data collected over time. The output at any given time is considered a function of the input signal, which is a function of time. Implicitly, we hope the input-output data approximated is sufficiently rich that the model will be accurate over a wide class of inputs and is useful for other purposes such as controlling the system. The recent advances in machine learning such as artificial neural network (ANN) can be used to find a global continuous map from system input space to system output space; however, the performance of these algorithms decreases drastically as the dimension of the system output vector increases. To make this point more

*Graduate Student, Department of Aerospace Engineering, The Pennsylvania State University, University Park, PA, 16802

†Senior Aerospace Engineer, AIAA Associate Fellow, AAS Fellow, Space Vehicles Directorate, Air Force Research Laboratory, Kirtland AFB, NM, 87117

‡Professor, AIAA Associate Fellow, AAS Fellow, Department of Aerospace Engineering, The Pennsylvania State University, University Park, PA, 16802

clear, consider the problem of active control of a flexible space structure. Generally, the system output vector consists of surface distortion measurements at various spatial points, $O(10^3)$, which are measured by sensors such as strain gauges, slope sensors, stereo vision systems, LIDAR, etc. Therefore, if one seeks a dynamic continuous map between the system output and input then the dimension of such a map can be as large as the number of measurements, i.e., $O(10^3)$. Conversely, the dimension of the hidden states, corresponding to the true system, corresponds to the number of dynamic structural modes of interest, which are typically less than 10. So, a system identification algorithm is desired that can approximate the system output accurately while keeping the dimension of the dynamic map as low as possible.

Flexible multibody systems have been a heavy research topic for decades. The work of Meirovich and Stemple¹⁶ from the mid 90s diverges away from classical approximations such as the Rayleigh-Ritz Method and finite element method. They instead present a mathematical formulation for distributed-parameter multibody systems which consists of ordinary and partial differential equations of motion in terms of quasicordinates.

In this paper, we will develop a dynamic model of the conceptual spacecraft via a Lagrangian method developed by Junkins and Kim² with the help of mathematical methods used by Dym and Shames.¹⁵ Junkins and Kim derived one-dimensional coupled rigid-elastic equations-of-motion in their work. We extend this to two dimensions. These coupled rigid-flexible equations of motion fully describe the motion and vibrational characteristics of the spacecraft over time. We then perform basic translational/rotational simulations to gain insight about the dynamics of the structure. Lastly, we study how the dynamics evolve for a case study of a sun-synchronous orbit. In future work, we will then utilize linear system identification tools such as the Eigensystem Realization Algorithm (ERA)^{8,9} to find the subspace over which the dynamics can be explained while approximating the input-output data collected from the distributed sensor arrays.

MATHEMATICAL BACKGROUND

The following section details how to obtain Lagrange's equations of motion for a two-dimensional coupled rigid-elastic system. The work is an extension of Junkins' and Kim's work on one-dimensional coupled rigid-elastic systems² and utilizes mathematical methods from the work of Dym and Shames.¹⁵

We begin by splitting the Lagrangian into three terms,

$$\mathcal{L} = L_D + \int_{\Omega} \hat{L} d\Omega + L_B \quad (1)$$

where Ω is the spatial domain occupied by the undeformed flexible body, L_D is the discrete portion of \mathcal{L} , \hat{L} is the Lagrangian density of the flexible body, and L_B is associated with boundary motions.

We wish to obtain the governing equations and boundary conditions for a rigid-elastic system with two spatial independent variables, x and y . The generalized rigid and elastic coordinates in the Lagrangian are given by q and w , respectively. Therefore, the elastic

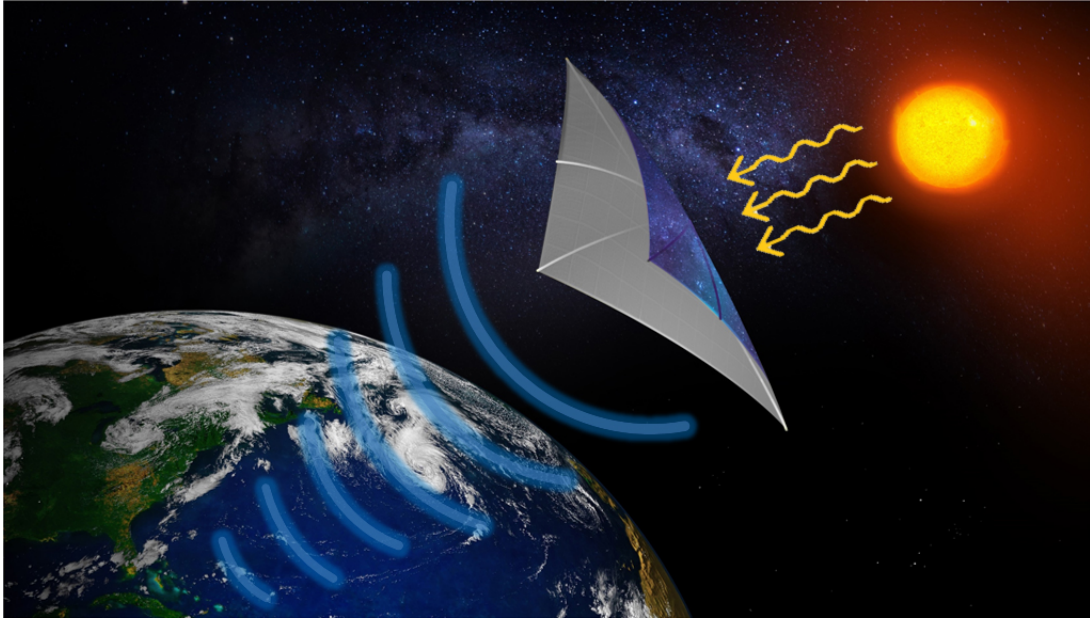


Figure 1: Conceptual Design of Spacecraft

deformation variable, w , is a function of x and y . As a result, both spatial derivatives must be accounted for in the Lagrangian. The following derivation is done in the (x, y) coordinate system due to its use in the next section; however, equations-of-motion and boundary conditions can be derived in any coordinate system. The Lagrangian shown in equation (1) now has the form

$$\mathcal{L} = L_D(q, \dot{q}) + \int \int_S \hat{L}(q, \dot{q}, w, \dot{w}, w_x, w_{xx}, w_y, w_{yy}, w_{xy}, w_{yx}) dA \quad (2)$$

$$+ L_B(q, \dot{q}, w, w_x, w_y, \dot{w}, \dot{w}_x, \dot{w}_y) \Big|_{\Gamma}$$

where $w_x = \frac{\partial w}{\partial x}$, $w_{xx} = \frac{\partial^2 w}{\partial x^2}$, $w_y = \frac{\partial w}{\partial y}$, $w_{yy} = \frac{\partial^2 w}{\partial y^2}$, $w_{xy} = \frac{\partial^2 w}{\partial x \partial y}$, and $w_{yx} = \frac{\partial^2 w}{\partial y \partial x}$. The variables S and Γ represent the the surface and boundary of the elastic domain, respectively. The corresponding boundary Lagrangian, \mathcal{L}_B , has its w components evaluated along this boundary. The nonconservative virtual work is given by,

$$\delta W_{nc} = Q^T \delta q + \int \int_S \hat{f}^T \delta w dA + \oint_{\Gamma} \left[f_1^T \delta w + f_2^T \delta w_x + f_3^T \delta w_y \right] dl \quad (3)$$

where Q is the generalized nonconservative force, \hat{f} is the nonconservative generalized force density vector associated with w , and $f_1^T - f_3^T$ are the nonconservative virtual works that depend on the boundary forces and associated boundary virtual displacements. To obtain the equations of motion, we wish to apply Hamilton's Principle. Therefore, we

carry out the variation of equation (2), add equation (3), and integrate over time to obtain:

$$\begin{aligned}
& \int_{t_1}^{t_2} (\delta\mathcal{L} + \delta W_{nc}) dt = \\
& \int_{t_1}^{t_2} \left\{ \frac{\partial L_D}{\partial q} \delta q + \frac{\partial L_D}{\partial \dot{q}} \delta \dot{q} + \frac{\partial L_B}{\partial q} \delta q + \frac{\partial L_B}{\partial \dot{q}} \delta \dot{q} + Q^T \delta q \right. \\
& + \int_{b_1}^{b_2} \int_{a_1}^{a_2} \left[\frac{\partial \hat{L}}{\partial q} \delta q + \frac{\partial \hat{L}}{\partial \dot{q}} \delta \dot{q} + \frac{\partial \hat{L}}{\partial \boldsymbol{\alpha}} \delta \boldsymbol{\alpha} + \frac{\partial \hat{L}}{\partial \dot{w}} \delta \dot{w} + \hat{f}^T \delta w \right] dx dy \\
& \left. + \frac{\partial L_B}{\partial \boldsymbol{\beta}} \delta \boldsymbol{\beta} \Big|_{\Gamma} + \frac{\partial L_B}{\partial \dot{\boldsymbol{\beta}}} \delta \dot{\boldsymbol{\beta}} \Big|_{\Gamma} + \oint_{\Gamma} [f_1^T \delta w + f_2^T \delta w_x + f_3^T \delta w_y] dl \right\} dt
\end{aligned} \tag{4}$$

where $\boldsymbol{\alpha} = [w, w_x, w_{xx}, w_y, w_{yy}, w_{xy}, w_{yx}]$ and $\boldsymbol{\beta} = [w, w_x, w_y]$. These variables are introduced to add brevity to the equation. In order to simplify this equation, we will utilize integration-by-parts and its two-dimensional counterpart derived from Gauss' Theorem.¹⁵ As a result, all variation variables that are differentiated will disappear and more boundary conditions will arise. The full simplification is omitted for brevity. Simplifying and setting to zero yields,

$$\int_{t_1}^{t_2} (\delta\mathcal{L} + \delta W_{nc}) dt = \int_{t_1}^{t_2} [A \delta q + B \delta w + C] dt = 0 \tag{5}$$

where,

$$\begin{aligned}
A &= \frac{\partial L_D}{\partial q} - \frac{d}{dt} \left(\frac{\partial L_D}{\partial \dot{q}} \right) + \int_{b_1}^{b_2} \int_{a_1}^{a_2} \left[\frac{\partial \hat{L}}{\partial q} - \frac{d}{dt} \left(\frac{\partial \hat{L}}{\partial \dot{q}} \right) \right] dx dy + \frac{\partial L_B}{\partial q} - \frac{d}{dt} \left(\frac{\partial L_B}{\partial \dot{q}} \right) + Q^T \\
B &= \int_{b_1}^{b_2} \int_{a_1}^{a_2} \left[\frac{\partial \hat{L}}{\partial w} - \frac{\partial}{\partial x} \left(\frac{\partial \hat{L}}{\partial w_x} \right) - \frac{\partial}{\partial y} \left(\frac{\partial \hat{L}}{\partial w_y} \right) + \frac{\partial^2}{\partial x^2} \left(\frac{\partial \hat{L}}{\partial w_{xx}} \right) + \frac{\partial^2}{\partial y^2} \left(\frac{\partial \hat{L}}{\partial w_{yy}} \right) \right. \\
& \left. + \frac{\partial}{\partial x} \frac{\partial}{\partial y} \left(\frac{\partial \hat{L}}{\partial w_{xy}} \right) + \frac{\partial}{\partial y} \frac{\partial}{\partial x} \left(\frac{\partial \hat{L}}{\partial w_{yx}} \right) - \frac{d}{dt} \left(\frac{\partial \hat{L}}{\partial \dot{w}} \right) + \hat{f}^T(x, y) \right] dx dy \\
C &= \frac{\partial L_B}{\partial \boldsymbol{\beta}} \delta \boldsymbol{\beta} \Big|_{\Gamma} - \frac{d}{dt} \left(\frac{\partial L_B}{\partial \dot{\boldsymbol{\beta}}} \delta \dot{\boldsymbol{\beta}} \right) \Big|_{\Gamma} + \oint_{\Gamma} [f_1^T \delta w + f_2^T \delta w_x + f_3^T \delta w_y] dl \\
& + \oint_{\Gamma} \left[\frac{\partial \hat{L}}{\partial w_x} - \frac{\partial}{\partial x} \left(\frac{\partial \hat{L}}{\partial w_{xx}} \right) - \frac{\partial}{\partial y} \left(\frac{\partial \hat{L}}{\partial w_{yx}} \right) \right] \delta w dx \\
& + \oint_{\Gamma} \left[\frac{\partial \hat{L}}{\partial w_y} - \frac{\partial}{\partial y} \left(\frac{\partial \hat{L}}{\partial w_{yy}} \right) - \frac{\partial}{\partial x} \left(\frac{\partial \hat{L}}{\partial w_{xy}} \right) \right] \delta w dy \\
& + \oint_{\Gamma} \frac{\partial \hat{L}}{\partial w_{xx}} \delta w_x dx + \oint_{\Gamma} \frac{\partial \hat{L}}{\partial w_{xy}} \delta w_y dx + \oint_{\Gamma} \frac{\partial \hat{L}}{\partial w_{yx}} \delta w_x dy + \oint_{\Gamma} \frac{\partial \hat{L}}{\partial w_{yy}} \delta w_y dy
\end{aligned} \tag{6}$$

In order for equation (5) to be satisfied, the three terms A , B , and C must be equal to zero individually. This is a typical argument used in this class of variational calculus problems. Utilizing equation (1), we can combine the L_D , \hat{L} , and L_B terms in A to obtain the standard Lagrange's equation shown in equation (7) below. Setting B equal to zero leads to the elastic domain equation (8).

$$\frac{d}{dt} \left(\frac{\partial \mathcal{L}}{\partial \dot{q}} \right) - \frac{\partial \mathcal{L}}{\partial q} = Q^T \quad (7)$$

$$\begin{aligned} \frac{d}{dt} \left(\frac{\partial \hat{L}}{\partial \dot{w}} \right) - \frac{\partial \hat{L}}{\partial w} + \frac{\partial}{\partial x} \left(\frac{\partial \hat{L}}{\partial w_x} \right) + \frac{\partial}{\partial y} \left(\frac{\partial \hat{L}}{\partial w_y} \right) - \frac{\partial^2}{\partial x^2} \left(\frac{\partial \hat{L}}{\partial w_{xx}} \right) - \frac{\partial^2}{\partial y^2} \left(\frac{\partial \hat{L}}{\partial w_{yy}} \right) \\ - \frac{\partial}{\partial x} \frac{\partial}{\partial y} \left(\frac{\partial \hat{L}}{\partial w_{xy}} \right) - \frac{\partial}{\partial y} \frac{\partial}{\partial x} \left(\frac{\partial \hat{L}}{\partial w_{yx}} \right) = \hat{f}^T \end{aligned} \quad (8)$$

In order to obtain the boundary conditions, one must set the many terms of C equal to zero.

We now have our set of equations of motion and boundary conditions for the two-dimensional elastic variable, w . In the next section, we will apply these equations to derive a model for the solar-powered spacecraft.

APPLICATION TO SPACECRAFT

Problem Setup

For this analysis, it will be assumed that the spacecraft consists of a rigid boundary structure with a flexible membrane clamped within it. We also assume that the spacecraft undergoes an external torque (τ_{ext}), an external force (\mathbf{F}_{ext}), and the membrane undergoes an external load (\hat{f}).

Figure (2) below displays the spacecraft, reference frames, and position vectors. The spacecraft is shown on the right with the center of mass symbol being *only for the mass of the rigid frame*, not including the flexible membrane. Doing so helps simplify the definition of the position vectors since the center of mass of the frame will be fixed relative to the body-fixed coordinates. The inertial reference frame $\{\hat{i}, \hat{j}, \hat{k}\}$ is given in the lower left in black, and the body-fixed reference frame $\{\hat{b}_1, \hat{b}_2, \hat{b}_3\}$ is given on the spacecraft in red. The two position vectors of interest are that of the rigid body's center of mass \mathbf{r}_{RB} (shown in green) and the position of any element on the membrane relative to the rigid body's center of mass \mathbf{r}_{Mem} (shown in blue).

Inertial \mathbf{r}_{RB} written in body-fixed coordinates is written generally as

$$\mathbf{r}_{RB} = X\hat{b}_1 + Y\hat{b}_2 + Z\hat{b}_3 \quad (9)$$

The position of any element of the membrane relative to inertial (\mathbf{r}_{Flex}) is written in terms of \mathbf{r}_{Mem} and \mathbf{r}_{RB} as

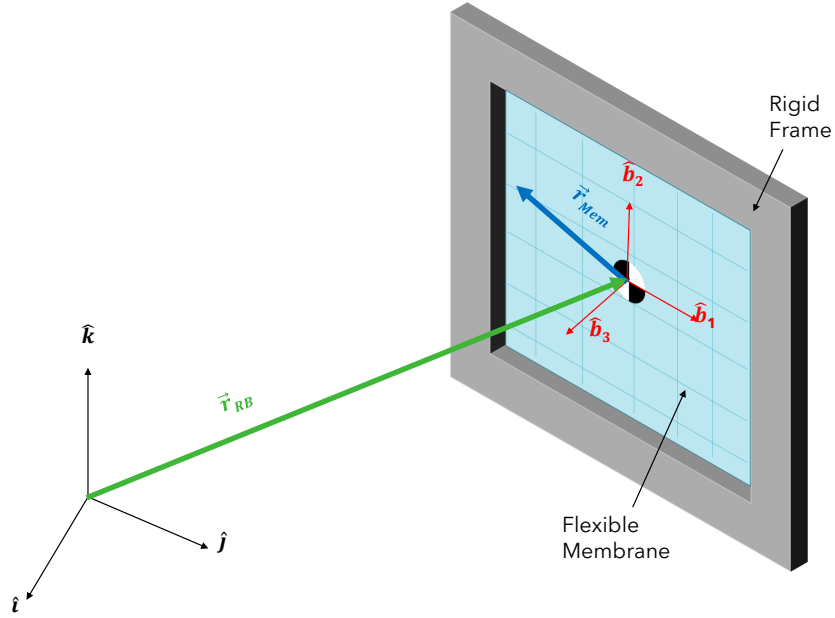


Figure 2: Spacecraft Frames and Position Vectors

$$\begin{aligned}
 \mathbf{r}_{Flex} &= \mathbf{r}_{RB} + \mathbf{r}_{Mem} \\
 \mathbf{r}_{Flex} &= \mathbf{r}_{RB} + x\hat{\mathbf{b}}_1 + y\hat{\mathbf{b}}_2 + \eta\hat{\mathbf{b}}_3 \\
 &= (X + x)\hat{\mathbf{b}}_1 + (Y + y)\hat{\mathbf{b}}_2 + (Z + \eta)\hat{\mathbf{b}}_3
 \end{aligned} \tag{10}$$

where $\{x, y, \eta\}$ are the positions of any membrane element relative to the rigid body center of mass in the $\{\hat{\mathbf{b}}_1, \hat{\mathbf{b}}_2, \hat{\mathbf{b}}_3\}$ reference frame, respectively. Note that what we are calling η is analogous to w in the derivation of the previous section (the use of w for the displacement is avoided here to prevent confusion with the angular velocity ω). For this derivation, only the displacement of the membrane in the $\hat{\mathbf{b}}_3$ direction, corresponding to η in equation (10), will be considered. Lateral displacements in the $\hat{\mathbf{b}}_1$ and $\hat{\mathbf{b}}_2$ directions will be neglected. This meaning that the membrane can only oscillate in the $\hat{\mathbf{b}}_3$ direction.

The angular velocity for the body is written as,

$$\boldsymbol{\omega} = \omega_1\hat{\mathbf{b}}_1 + \omega_2\hat{\mathbf{b}}_2 + \omega_3\hat{\mathbf{b}}_3 \tag{11}$$

The time derivatives of the position vectors are then,

$$\dot{\mathbf{r}}_{RB} = \nu_1\hat{\mathbf{b}}_1 + \nu_2\hat{\mathbf{b}}_2 + \nu_3\hat{\mathbf{b}}_3 \tag{12}$$

$$\begin{aligned}
\dot{\mathbf{r}}_{Flex} &= \nu_1 \hat{\mathbf{b}}_1 + \nu_2 \hat{\mathbf{b}}_2 + (\nu_3 + \dot{\eta}) \hat{\mathbf{b}}_3 + \boldsymbol{\omega} \times (x \hat{\mathbf{b}}_1 + y \hat{\mathbf{b}}_2 + \eta \hat{\mathbf{b}}_3) \\
&= (\nu_1 + \omega_2 \eta - \omega_3 y) \hat{\mathbf{b}}_1 + (\nu_2 + \omega_3 x - \omega_1 \eta) \hat{\mathbf{b}}_2 \\
&\quad + (\nu_3 + \dot{\eta} + \omega_1 y - \omega_2 x) \hat{\mathbf{b}}_3
\end{aligned} \tag{13}$$

where ν_1, ν_2 , and ν_3 are quasi-velocities (i.e. inertial velocities written in body-fixed coordinates).

It's important to note here that, since we are using quasi-velocities for our \mathbf{r}_{RB} vector, there is no need to apply the transport theorem when taking a time derivative; however, since \mathbf{r}_{Mem} is a part of the definition of the \mathbf{r}_{Flex} vector, and \mathbf{r}_{Mem} is *not* defined to be inertial, the transport theorem *does* have to be applied when taking the time derivative of \mathbf{r}_{Flex} . We are also using quasi-velocities when it comes to the angular velocity since we have not included any Euler angles.

Lagrangian

Now, with the velocities defined, one can write the kinetic and potential energies of the system as,

$$T = \frac{1}{2} \boldsymbol{\omega}^T I \boldsymbol{\omega} + \frac{1}{2} M_{RB} (\dot{\mathbf{r}}_{RB} \cdot \dot{\mathbf{r}}_{RB}) + \int_{b_1}^{b_2} \int_{a_1}^{a_2} \frac{1}{2} \rho (\dot{\mathbf{r}}_{Flex} \cdot \dot{\mathbf{r}}_{Flex}) dx dy \tag{14}$$

$$V = \int_{b_1}^{b_2} \int_{a_1}^{a_2} \frac{1}{2} P (\nabla \eta \cdot \nabla \eta) dx dy \tag{15}$$

Where I is the inertia matrix (this derivation will assume that the body-fixed axes are aligned with the principle inertia axes), M_{RB} is the total mass of the rigid frame, ρ is the density per unit area of the membrane, and P is the tension within the membrane. Substituting equations (12) and (13) into $T - V$ yields the following Lagrangian:

$$\begin{aligned}
\mathcal{L} &= \frac{1}{2} \boldsymbol{\omega}^T I \boldsymbol{\omega} + \frac{1}{2} M_{RB} (\nu_1^2 + \nu_2^2 + \nu_3^2) + \int_{b_1}^{b_2} \int_{a_1}^{a_2} \left[\frac{1}{2} \rho \left((\nu_1 + \omega_2 \eta - \omega_3 y)^2 \right. \right. \\
&\quad \left. \left. + (\nu_2 + \omega_3 x - \omega_1 \eta)^2 + (\nu_3 + \dot{\eta} + \omega_1 y - \omega_2 x)^2 \right) - \frac{1}{2} P (\nabla \eta \cdot \nabla \eta) \right] dx dy
\end{aligned} \tag{16}$$

Equations of Motion

From equation (16), it can be seen that our generalized coordinates, \mathbf{q} , of our Lagrangian are the translation velocity, $\boldsymbol{\nu}$, and the angular velocity, $\boldsymbol{\omega}$. These quantities are quasi-velocities. As a result of using quasi-velocities in our Lagrangian formulation, we must utilize the following modified form of equation (7),¹⁴

$$\frac{d}{dt} \left(\frac{\partial \mathcal{L}}{\partial \nu_k} \right) + \omega_{kj}^\times \frac{\partial \mathcal{L}}{\partial \nu_j} = F_k \tag{17}$$

$$\frac{d}{dt} \left(\frac{\partial \mathcal{L}}{\partial \omega_k} \right) + \omega_{kj}^\times \frac{\partial \mathcal{L}}{\partial \omega_j} = Q_k \tag{18}$$

Note that equations (17) and (18) are written in index notation. Applying equation (17) to the Lagrangian in equation (16), simplifying with heavy matrix algebra, and then interpreting matrix multiplications as vector products yields the following vector equation,

$$M_{RB}(\ddot{\mathbf{r}}_{RB} + \boldsymbol{\omega} \times \dot{\mathbf{r}}_{RB}) + \int_{b_1}^{b_2} \int_{a_1}^{a_2} \rho(\ddot{\mathbf{r}}_{Flex})dxdy = \mathbf{F}_{Ext} \quad (19)$$

Performing the same process for equation (18) yields,

$$I\dot{\boldsymbol{\omega}} + \boldsymbol{\omega} \times (I\boldsymbol{\omega}) + \int_{b_1}^{b_2} \int_{a_1}^{a_2} \rho \left\{ \mathbf{r}_{Mem} \times (\ddot{\mathbf{r}}_{Mem} + \ddot{\mathbf{r}}_{RB}) + \dot{\mathbf{r}}_{Mem} \times \dot{\mathbf{r}}_{RB} \right\} dxdy = \boldsymbol{\tau}_{Ext} \quad (20)$$

Lastly, applying the same process with the elastic domain equation (8) yields,

$$\int_{b_1}^{b_2} \int_{a_1}^{a_2} [\rho(\ddot{\mathbf{r}}_{Flex}) \cdot \hat{\mathbf{b}}_3 - P\nabla^2\eta]dxdy = \int_{b_1}^{b_2} \int_{a_1}^{a_2} \hat{f}dxdy \quad (21)$$

Setting the integrands equal,

$$\rho(\ddot{\mathbf{r}}_{Flex}) \cdot \hat{\mathbf{b}}_3 - P\nabla^2\eta = \hat{f} \quad (22)$$

Equation (22) is of the form of the well-known, clamped-boundary-condition membrane equation: $\rho\ddot{u} - P\nabla^2u = \hat{f}$ where u is the displacement of the membrane. Obtaining this result makes intuitive sense because the membrane is clamped within the rigid boundary structure.

Equations (19), (20), and (22), are the full set of equations of motion for the model spacecraft.

Solving Membrane Partial Differential Equation

We approximate the displacement of the membrane, η , by assuming a separation of spatial and time variables within the following summation,

$$\eta(x, y, t) = \sum_{i=1}^N \phi_i(x, y)q_i(t) \quad (23)$$

where $\phi_i(x, y)$ are chosen basis functions, $q_i(t)$ are the corresponding modal amplitudes, and N is the number of basis functions. For the rigid body equations (20) and (19), the above equation can be directly substituted. For the partial differential, membrane equation (22), we must apply a weighted residuals method. We choose to apply the Galerkin Method of Weighted Residuals.

Method of Weighted Residuals: Galerkin Method In general, consider a linear differential operator D acting on a function u to produce a function p ,

$$D(u(x, y)) = p(x, y) \quad (24)$$

We wish to approximate the function u using our assumed modes method,

$$u \cong \tilde{u} = \sum_{i=1}^N \phi_i(x, y) q_i(t) \quad (25)$$

When substituted into the differential, D , the result of the operations is not, in general, $p(x)$. Therefore, an error, or residual, will exist,

$$E(x, y) = R(x, y) = D(\tilde{u}(x, y)) - p(x, y) \neq 0 \quad (26)$$

We wish to force the residual to zero in an average over the domain. That is,

$$\int_{b_1}^{b_2} \int_{a_1}^{a_2} R(x, y) W_i dx dy = 0 \quad i = 1, 2, \dots, N \quad (27)$$

There are many different methods for choosing the weightings, W_i . For our purposes, we will be using the Galerkin method where the weightings are equal to the original basis functions,

$$W_i = \frac{\partial \tilde{u}}{\partial q_i} = \phi_i(x, y) \quad (28)$$

This leads to equation (22) becoming a system of N ordinary differential equations instead of one partial differential equation. After applying equation (25) to equation (22), the residual is found to be:

$$R = \rho[\dot{\nu}_3 + (\phi_i \ddot{q}_i) + \dot{\omega}_1 y - \dot{\omega}_2 x - \nu_1 \omega_2 + (-\omega_2^2 - \omega_1^2)(\phi_i q_i) \quad (29)$$

$$+ \omega_3 \omega_2 y + \omega_1 \nu_2 + \omega_1 \omega_3 x] - P[\phi_{xx_i} q_i + \phi_{yy_i} q_i] - \hat{f} \quad (30)$$

Substituting the above residual into equation (27) yields,

$$\int_{b_1}^{b_2} \int_{a_1}^{a_2} \left[\rho[\dot{\nu}_3 + (\phi_i \ddot{q}_i) + \dot{\omega}_1 y - \dot{\omega}_2 x - \nu_1 \omega_2 + (-\omega_2^2 - \omega_1^2)(\phi_i q_i) \right. \\ \left. + \omega_3 \omega_2 y + \omega_1 \nu_2 + \omega_1 \omega_3 x] - P[\phi_{xx_i} q_i + \phi_{yy_i} q_i] - \hat{f} \right] \phi_j dx dy = 0 \quad (31) \\ j = 1, 2, \dots, N$$

Where the $\phi_i q_i$ terms are the full summation defined in equation (25) and ϕ_j is the weighting function for the j^{th} assumed mode corresponding to the j^{th} equation in the N equation system of obtained via the Galerkin Method. We now have a system of ordinary differential equations in time with variables $\nu_1, \nu_2, \nu_3, \omega_1, \omega_2, \omega_3$, and q . In the next section, we will solve these equations over time for different external loadings.

NUMERICAL SOLUTIONS OF EQUATIONS OF MOTION

We are now ready to simulate results for our model. For this problem, the modes of a clamped-clamped membrane that is stationary will be used as the basis functions in the assumed modes analysis. These modes are,

$$\phi_{ij}(x, y) = \sin\left[\frac{i\pi}{a}\left(x - \frac{a}{2}\right)\right] \sin\left[\frac{j\pi}{b}\left(y - \frac{b}{2}\right)\right] \quad i, j = 1, 2, \dots, N \quad (32)$$

where a and b are the width and height of the rectangular membrane, respectively. The work in the previous section had singular index notation, but our basis functions require two indices. The notation is modified to,

$$\begin{aligned} \phi_i(x, y) &:= \phi_{ij}(x, y) \\ \phi_j(x, y) &:= \phi_{mn}(x, y) \end{aligned}$$

where all indices go from 1 to N .

For the following examples of output data, the following physical parameters were used:

N	a	b	ρ	P	M_{RB}	I
4	10 m	10 m	$5 \frac{kg}{m^2}$	200 N	100 kg	$\begin{bmatrix} 33.667 & 0 & 0 \\ 0 & 33.667 & 0 \\ 0 & 0 & 67.333 \end{bmatrix} kgm^2$

As a result, η is defined as:

$$\begin{aligned} \eta = & \sin\left[\frac{\pi(x-5)}{10}\right] \sin\left[\frac{\pi(y-5)}{10}\right] q_1(t) \\ & + \sin\left[\frac{\pi(x-5)}{10}\right] \sin\left[\frac{\pi(y-5)}{5}\right] q_2(t) \\ & + \sin\left[\frac{\pi(x-5)}{5}\right] \sin\left[\frac{\pi(y-5)}{10}\right] q_3(t) \\ & + \sin\left[\frac{\pi(x-5)}{5}\right] \sin\left[\frac{\pi(y-5)}{5}\right] q_4(t) \end{aligned}$$

The following two subsections showcase results for the fully-coupled model derived in this paper and a decoupled model. The fully-coupled model numerically integrates all equations of motion simultaneously for a given external force/torque. The goal of the fully-coupled results is to examine how the dynamics evolve in basic translation/rotation motion. This will help to gain more of an intuitive understanding of the dynamics.

The decoupled model is utilized for simulating the membrane's response in-orbit. The decoupling allows the dynamics of the rigid body to affect the membrane, but not vice-versa. This is necessary due to numerical issues that arise when attempting to integrate the

fully-coupled model in-orbit. The decoupled model is described by the flowchart in Figure (3). First, the position and translational velocity are obtained over time from a simple point-mass Earth gravity model and the angular velocity is obtained from Euler's rigid-body rotation equations. Next, the angular velocities are utilized in the differential equations for attitude quaternions so that the direction-cosine matrix (DCM) can be determined. With this DCM, the inertial velocity in the body fix frame, ν , is calculated. Finally, the position, ν , and ω are fed into the membrane dynamics to determine the modal amplitude over time.

Note that the same system parameters are used for both models.

Fully-Coupled Model Results

In Figure (4a), an external force of magnitude 0.001 N, only in the \hat{b}_3 direction, is applied to the spacecraft for 10 seconds. There are no external torques or distributed loads applied. It is important to note that, by definition, this force is applied evenly on the rigid frame, not the membrane itself. The first mode of the membrane is excited due to this acceleration and the modal amplitude has a sinusoidal response. This response is due to the inertia of the spacecraft causing a "sag" in the membrane as it begins to translate due to the external force. As this is happening, the strain energy of the membrane creates an acceleration that counters this sag until the membrane "rebounds" and becomes flat again. This cycle continues on as the spacecraft translates. The velocity in the \hat{b}_3 direction (ν_3) is increasing as expected, but with slight fluctuations. This is due to the aforementioned vibration of the membrane.

In Figure (4b), a constant torque of 0.001 Nm is applied about the \hat{b}_1 and \hat{b}_2 axes. There are no external forces or distributed loads applied. The rotational velocities ω_1 and ω_2 have slightly nonlinear trends due to the vibration of the membrane as described from the results of Figure (4a). Two modes were excited in this case and followed different sinusoidal waves. No translational velocity occurred due to the specific mode shapes that were excited. Modes (1,2) and (2,1) oscillate with an even amount of mass displaced relative to the \hat{b}_1 - \hat{b}_2 plane. This meaning there is no net force acting on the satellite at any time during this vibration. This is not true for the mode (1,1) that was induced in the results of Figure (4a).

In Figure (4c), a constant force of 0.001 N is applied in the \hat{b}_1 and \hat{b}_2 directions and a constant torque of 0.001 Nm is applied about the \hat{b}_3 axis. No distributed loads are applied. In this case, the translational velocities ν_1 and ν_2 increase linearly with time. The rotational velocity ω_3 also increases linearly with time. This was expected since there was constant forcing and torquing in this case. No modes were ever excited, meaning that no vibration of the membrane occurred. This is due to our previous assumption when formulating the equations-of-motion that translational vibrations in the \hat{b}_1 and \hat{b}_2 directions would be ignored. These results showcase how external forces in the \hat{b}_1 and \hat{b}_2 directions and external torques in the \hat{b}_3 direction do not excite any modes in the membrane.

Decoupled Model Results

Figure (5) details the sun-synchronous orbit that will be used for our simulation. Two cases will be considered in this orbit: no torque and sinusoidal torque. The former is to

study if any modes will be excited during the orbit regardless of the spacecraft's rotation, and the latter is to study the modes excited with rotation on-top of orbital dynamics.

The results shown in Figure (6) display that only the first mode of the membrane is activated during the orbit when no external torque is present on the spacecraft. The spacecraft started with no angular velocity and the body-frame was aligned with inertial. The modal amplitude of this mode peaks at a magnitude greater than one. This means that, for our spacecraft parameters, the membrane is experiencing large displacements from its resting position. This may indicate that the decoupled assumption is not valid. This of course depends heavily on the parameters of the spacecraft.

For the final case in Figure (7) where a sinusoidal external torque of amplitude 0.001 Nm (about all 3 axes) was applied on-top of the orbital dynamics, a similar trend to the previous example occurred. The first mode had the same trend with slight fluctuations, but the second and third modes were activated slightly as well. The magnitude of the second and third modes was much smaller than that of the first mode. It seemed that, although more modes were activated when an external torque was introduced, the dominate mode occurred from the orbital dynamics rather than the rigid-body rotation. This of course depends heavily on the parameters of the spacecraft as well.

CONCLUSIONS AND FUTURE WORK

In this paper, the ground work was laid for the derivation of equations-of-motion of a coupled rigid-flexible spacecraft structure. First, Junkins' and Kims'² work in one-dimensional equations-of-motion was extended to two-dimensions for a general coupled rigid-flexible system. Then, a model was defined for the spacecraft and relevant position vectors were introduced. From there, the model was applied to the two-dimensional equations and equations-of-motion were obtained for the spacecraft. In total, there were 7 equations: three Newton's second law ($F = ma$) equations, three Euler's rigid-body rotation equations, and one membrane equation. With this system of equations, the dynamics of the spacecraft in orbit can now be solved. A preliminary analysis was performed by solving the membrane equation via the Galerkin method of weighted residuals. Solving these equations numerically for different external forces yielded intuitive results of the membrane's dynamics thus giving optimism for the formulation. A preliminary simulation of the spacecraft in a sun-synchronous orbit yielded useful vibrational results that could be used for structural analysis.

Further work can be done in modeling the spacecraft more accurately such modeling the elastic domain as a plate rather than a membrane. There is also work to do in improving the numerical efficiency when solving the differential equations of motion so that decoupling the model is not necessary.

ACKNOWLEDGEMENT

This material is based upon work supported by the space scholar program from AFRL space directorate.

REFERENCES

- ¹ “Space Solar Power Incremental Demonstrations and Research Project (SSPIDR)”, afresearchlab.com/technology/successstories/space-power-beaming/.
- ² J. Junkins and Y. Kim, *Introduction to Dynamics and Control of Flexible Structures*, American Institute of Aeronautics and Astronautics, Inc., pp. 139-225, 1993.
- ³ B. Ho and R. Kalman, *Effective Construction of Linear State Variable Models from Input/Output Data*, Proceedings of the 3rd Annual Allerton Conference on Circuit and System Theory, pp. 449-459, 1965.
- ⁴ A. Tether, *Construction of Minimal Linear State-Variable Models from Finite Input-Output Data*, IEEE Transactions on Automatic Control, Vol. AC-15, No. 4, pp. 427-436, Aug. 1970
- ⁵ Silverman, L.M., *Realization of Linear Dynamical Systems*, IEEE Transactions on Automatic Control, Vol. AC-16, No. 6, 1971, pp. 554-567.
- ⁶ R. Rossen and L. Lapidus, *Minimum Realizations and System Modeling: I. Fundamental Theory and Algorithms*, AIChE Journal, Vol. 18, No. 4, July 1972, pp. 673-684.
- ⁷ R. Rossen and L. Lapidus, *Minimum Realizations and System Modeling: II. Theoretical and Numerical Extensions*, AIChE Journal, Vol. 18, No. 5, Sept. 1972, pp. 881-892.
- ⁸ J. Juang, *Applied System Identification*, Prentice Hall, Englewood Cliffs, NJ, 1994, pp. 121–227.
- ⁹ J. Juang and R. Pappa, *An Eigensystem Realization Algorithm for Modal Parameter Identification and Model Reduction*, AIAA Journal of Guidance, Control, and Dynamics, 1984.
- ¹⁰ J. Turner and H. Chun, *Optimal Distributed Control of a Flexible Spacecraft During a Large-Angle Maneuver*, AIAA Journal of Guidance, Control, and Dynamics, 1984.
- ¹¹ N. Osikowicz and P. Singla, *Model-based Control of Tendon-Actuated Tensegrity Robots*, AIAA Region I Student Conference, 2021.
- ¹² J. Juang et al., *Identification of Observer/Kalman Filter Markov Parameters: Theory and Experiments*, AIAA Journal of Guidance, Control, and Dynamics, 1993.
- ¹³ M. Majji, J. Juang and J. Junkins, *Time-Varying Eigensystem Realization Algorithm*, AIAA Journal of Guidance, Control, and Dynamics, 2010.
- ¹⁴ Hurtado, J. E. and Sinclair, A. J. *Hamel Coefficients for the Rotational Motion of a Rigid Body* Proceedings of the Royal Society of London. Series A: Mathematical, Physical and Engineering Sciences, vol. 460, no. 2052, pp. 3613–3630, Dec. 2004.
- ¹⁵ Clive L. Dym and Irving H. Shames, *Solid Mechanics: A Variational Approach* A Variational Approach, McGraw-Hill Book Company, New York, 1973.
- ¹⁶ Meirovitch, L., and T. Stemple. ”Hybrid equations of motion for flexible multibody systems using quasi-coordinates.” *Journal of Guidance, Control, and Dynamics* 18.4 (1995): 678-688.

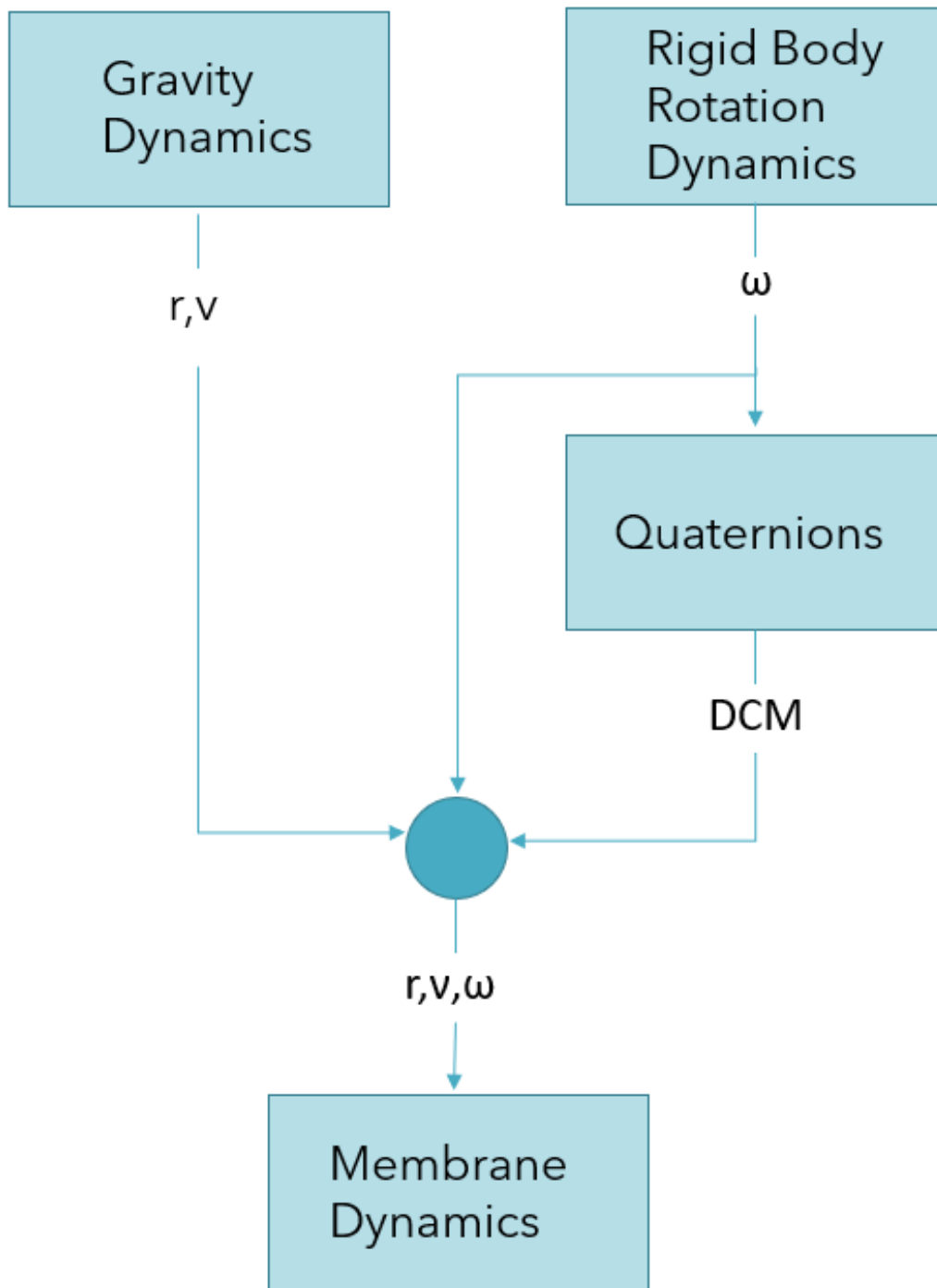
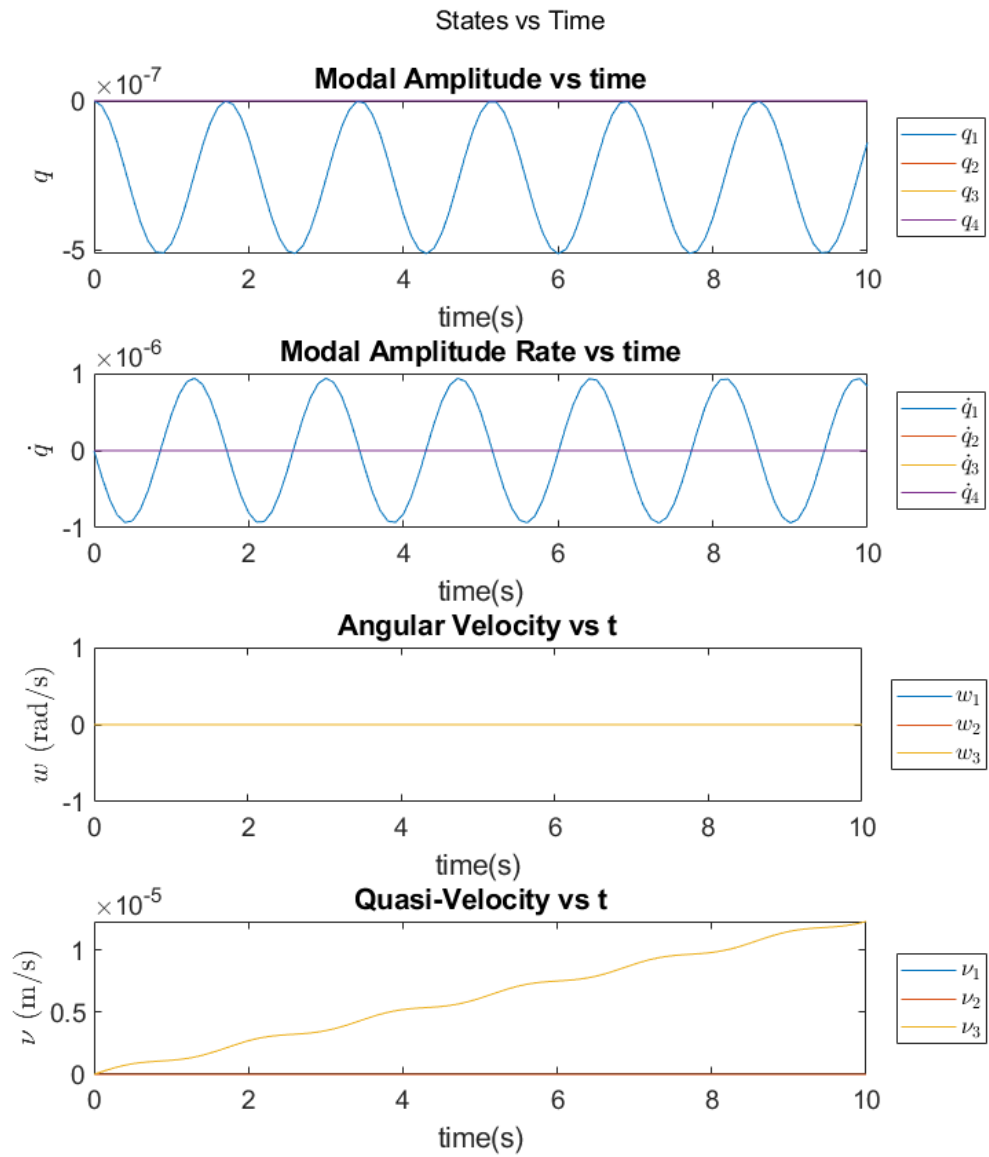
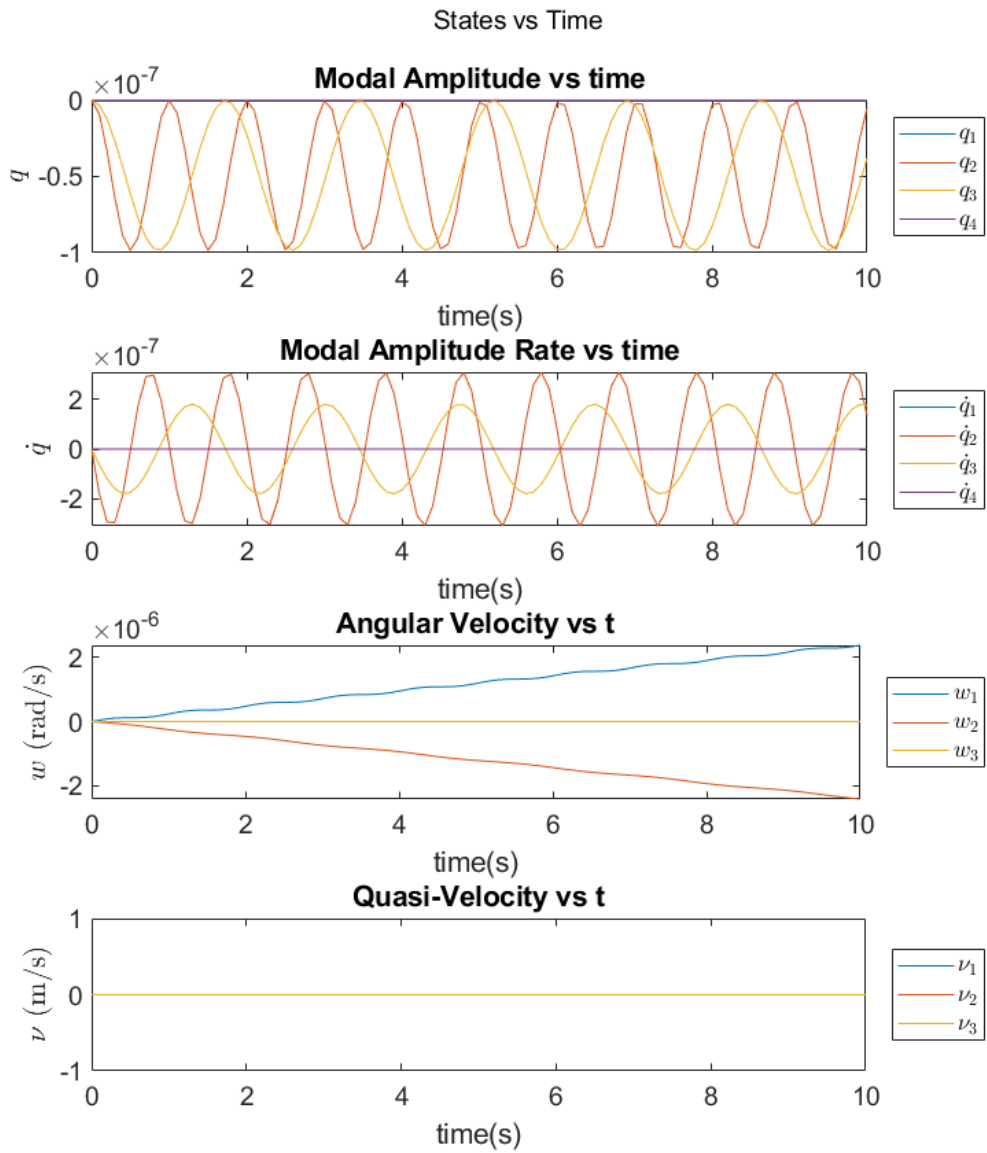


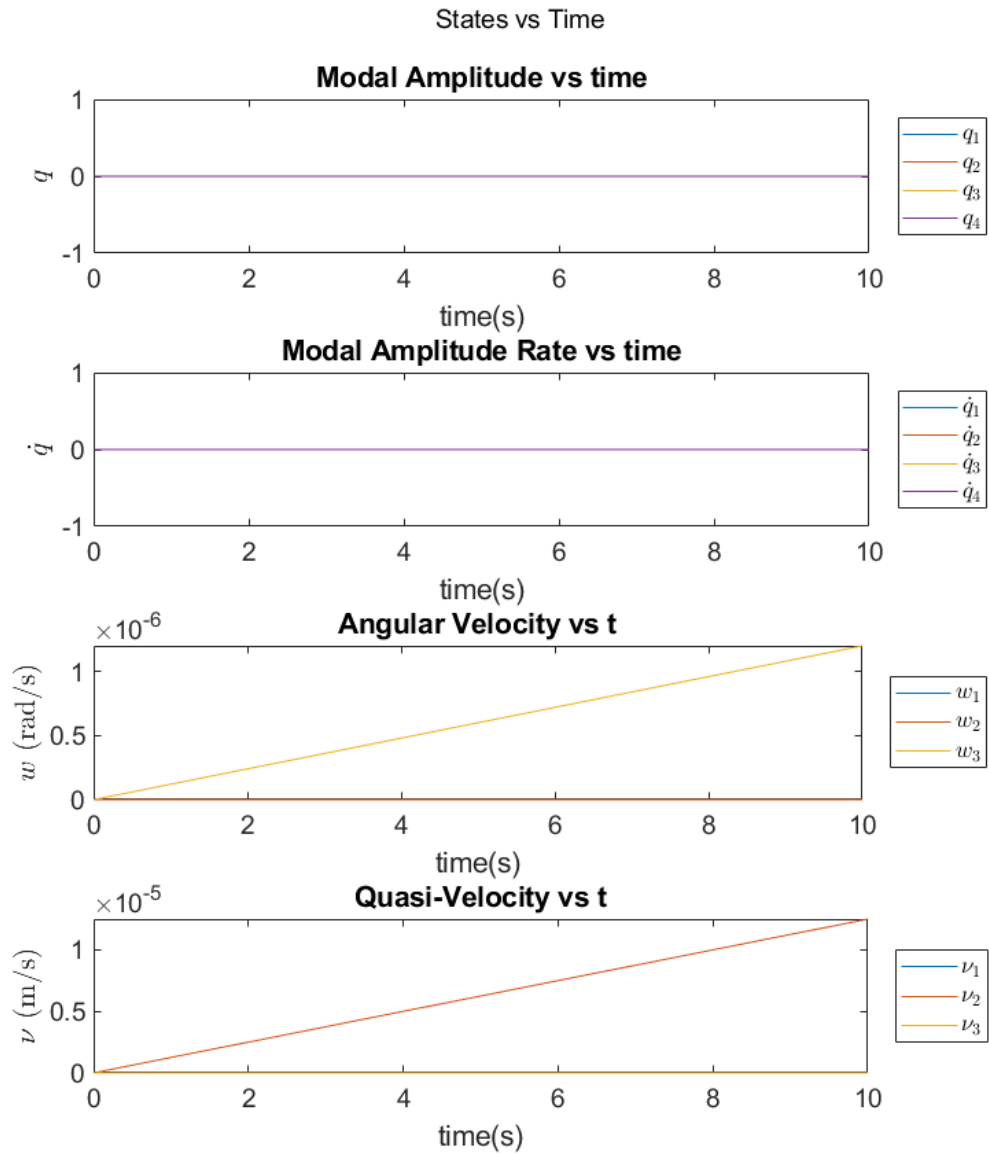
Figure 3: Decoupled Model Flowchart



(a) $\mathbf{F} = [0;0;0.001]$ N



(b) $\tau = [0.001; 0.001; 0]$ Nm



(c) $F = [0.001; 0.001; 0]$ N, $\tau = [0; 0; 0.001]$ Nm

Figure 4: Preliminary Results

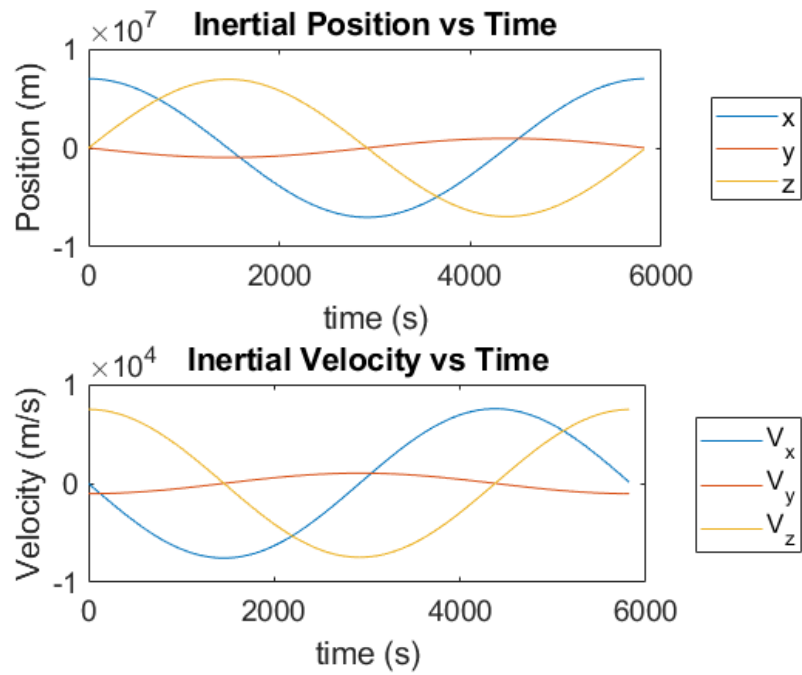
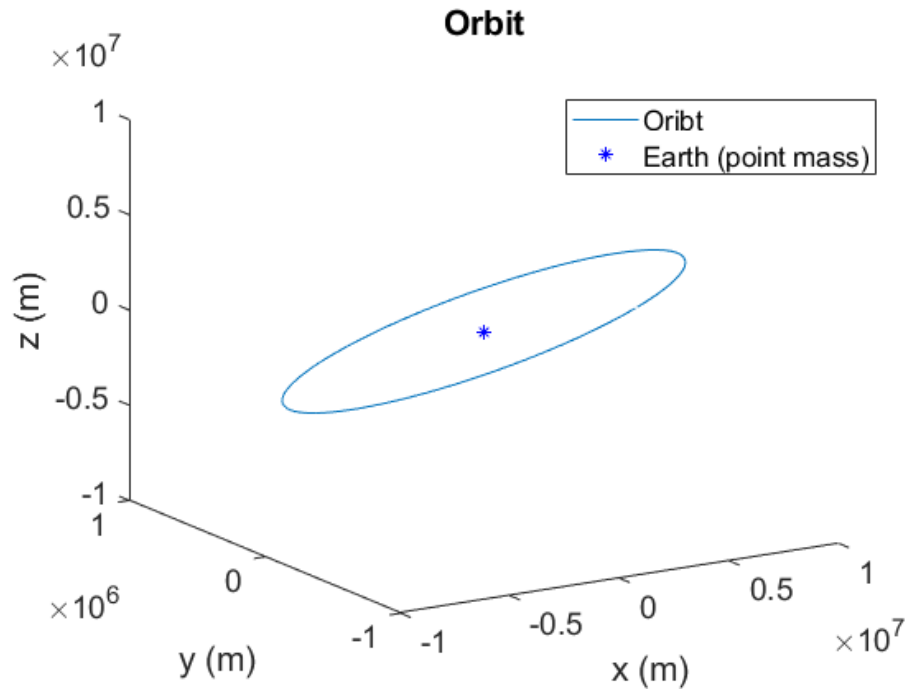


Figure 5: Sun-Synchronous Orbit

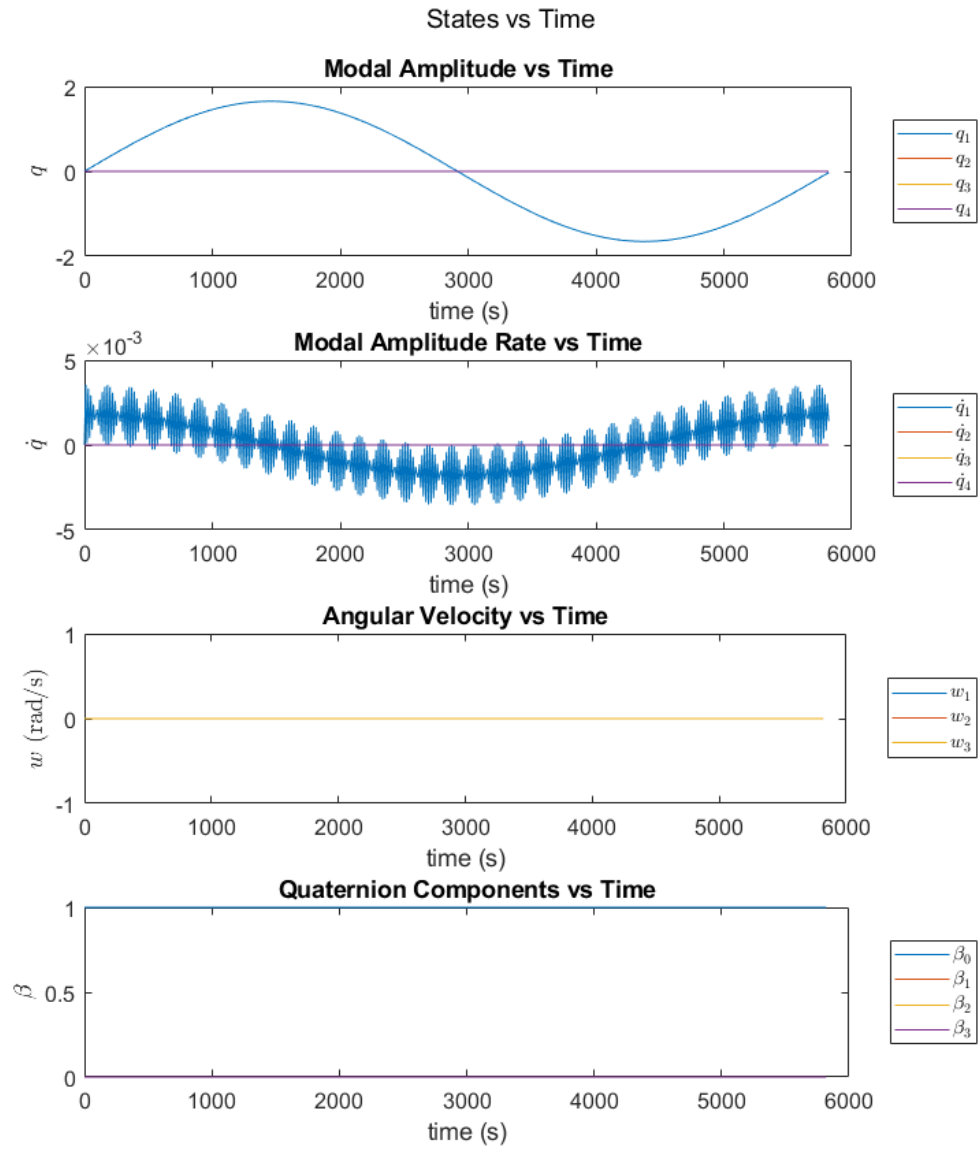


Figure 6: Torque-Free Response

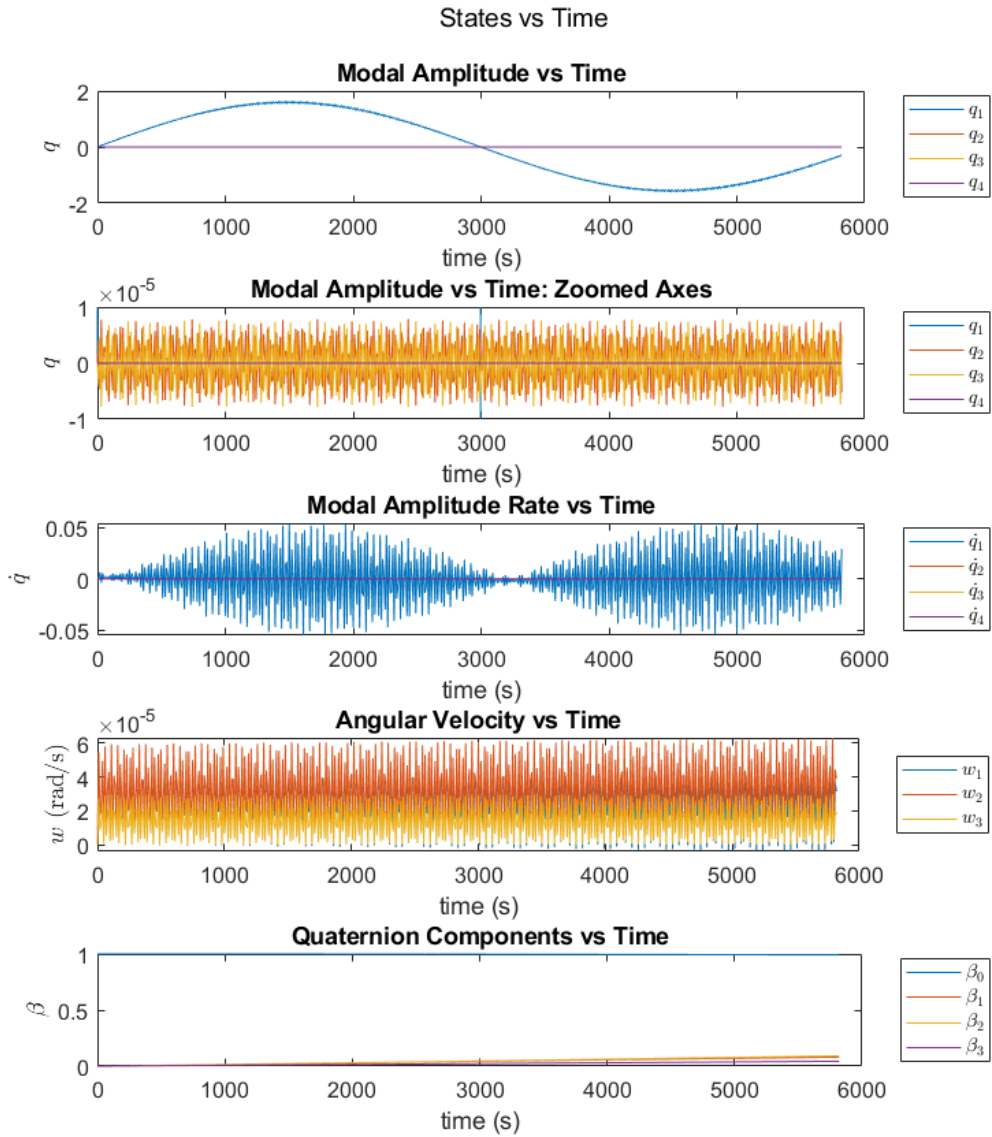


Figure 7: Torque Response: $\tau = 0.001 * [\sin(t); \sin(t); \sin(t)]$ Nm